ICSV13 - Vienna
The Thirteenth International Congress on Sound and Vibration
Vienna, Austria, July 2-6, 2006

AEROACOUSTICS OF FLOW DUCT WITH MULTIPLE CAVITIES

R. C. K. Leung[1], R. M. C. So[1] and S. K. Tang[2]

[1]Department of Mechanical Engineering, The Hong Kong Polytechnic University
Hung Hom, Kowloon, Hong Kong, China
[2]Department of Building Services Engineering, The Hong Kong Polytechnic University
Hung Hom, Kowloon, Hong Kong, China
mmrleung@inet.polyu.edu.hk

Abstract

The objective of this paper is to verify the concept of passive noise reduction in an in-duct device (cavity) through enhancement of noise interference. Design requirements and space limitations often cause the flow to change direction, thus leading to branching and the necessity of introducing in-duct devices, which will invariably affect the flow and acoustics inside the ductworks. Turbulence, and consequently noise, is also generated at these in-duct devices. A simple yet common form of in-duct device is a cavity. Aeroacoustic behavior of an open cavity is strongly dependent on the fluid-resonant behavior within the cavity. The shear layer resonates at Rossiter frequencies and drives the acoustic wave propagation towards the upstream far field. However, in such realistic applications as gas transport systems, the cavity does not exist alone but is enclosed by solid walls and/or surrounded by different kinds of in-duct devices. The flow-resonant behavior and noise radiation of a cavity is altered. Even though each in-duct device would generate its own noise, possibilities exist that the devices could be properly arranged so as to strengthen noise interference, thus leading to less overall noise radiation in the in-duct far field. This possibility of noise control in in-duct devices is investigated in the present study. A two dimensional approach is adopted and duct aeroacoustics is calculated by means of a one-step aeroacoustics simulation based on finite difference direct numerical simulation (DNS) technique. An additional cavity located on the opposite duct wall is used as the controlling device. The position of the additional cavity is varied. Its dimensions and relative locations are varied and the resultant aeroacoustics behavior is assessed. It was found that a 7.9 db reduction of noise power is possible with an offset of one-half cavity length.

INTRODUCTION

Noise control of flow through a duct is a very important issue in many engineering applications, such as automobile industry, ventilation duct and exhaust pipe, etc. There are two major types of noise generation mechanisms. The first type is the interaction between vortices in shear layers emanating from structural discontinuities or in the wake behind immersed structures in duct flows. The second type is the interaction between vortices and solid boundaries of structural discontinuities, which appear as a result of installation of flow management devices in ducts. Acoustic waves are generated when the unsteady flow passes over gaps or obstacles inside a duct. The interaction becomes even more complicated if aeroacoustic resonance occurs in the ductworks. Therefore, it is a common objective for engineers to minimize the noise level generated by the unsteady flow past flow in-duct devices. This is particularly important for high-pressure gas transport because the resonant high-pressure oscillations could be a possible excitation source of flow-induced vibration of the duct works and their eventual failure due to fatigue.

A simple yet common form of in-duct device is a cavity. Noise generation from the flow past an open cavity is strongly dependent on the fluid-resonant behaviour within the cavity. The shear layer resonates at Rossiter frequencies and drives the acoustic wave propagation towards the upstream far field. A great deal of experimental and numerical works have been carried out [1–3] for a better understanding of the open cavity noise mechanism. In such realistic applications as gas transport systems, the cavity, however, does not exist alone but is enclosed by solid walls and/or surrounded by different kinds of in-duct devices. The flow-resonant behaviour and noise radiation of a cavity is greatly altered as a result. Even though each in-duct device would generate its own noise, possibilities exist that the devices could be properly arranged to strengthen noise interference so that a net overall reduction of noise radiation in the in-duct far field could be achieved. This possibility of passive control of noise by enhancing noise interference due to duct devices is investigated in the present study. An in-duct cavity is used as an example. Additional cavity located on the opposite wall is used as a controlling device. The locations of the cavities are varied and the resultant aeroacoustics behaviour is assessed.

One-step aeroacoustic simulation is the preferred simulation methodology as this scheme is able to accurately resolve the far-field aeroacoustic disturbances, near-field unsteady flows, and their interactions, simultaneously. The methodology is successful in simulating aeroacoustics of open flows. One-step simulation usually calls for a low dispersive and low dissipative finite-difference DNS scheme in order to capture accurately the acoustic fluctuations, the magnitudes of which are at least three orders of magnitude smaller than the associated flow fluctuations. High-order schemes are usually required so as to suppress the magnitude of truncation errors to well below those of acoustics. In addition, the treatment of inflow and outflow boundary conditions does have significant effect on the accuracy of aeroacoustic simulations. Buffer regions are usually required at the inlet and outlet boundaries so as to allow the unsteady flow field to pass through them with minimal reflection of all outgoing acoustic waves. In the present study, the one-step aeroacoustic simulation using DNS is extended to calculate duct aeroacoustics and their passive noise control.

THEORETICAL FORMULATION AND NUMERICAL SCHEME

Figure 1 illustrates the computational domain of the basic configuration of a laminar flow through a duct containing an in-duct cavity. In the forgoing discussion this configuration is denoted as *BD*. The width of the two-dimensional flow duct is *W*. An in-duct cavity of depth *H* and length *L* is installed at the bottom wall of the duct. The cavity dimensions are specified as $L/H=2$ and $W/H=2$, where H is the cavity height, L its length and W is the height of the duct. The length of the duct under consideration is $-3 \le x/H \le 7$. The governing equations are the unsteady, compressible, Navier-Stokes equations in two dimensions. Written in strong conservation form, they are represented in Cartesian coordinates (x, y) as

$$\frac{\partial \mathbf{Q}}{\partial t}+\frac{\partial \mathbf{E}}{\partial x}+\frac{\partial \mathbf{F}}{\partial y}=\mathbf{S}_v=\frac{\partial \mathbf{E}_v}{\partial x}+\frac{\partial \mathbf{F}_v}{\partial y} \quad , \tag{2}$$

where the conservative variables and the inviscid flux vectors are given by

$$\mathbf{Q}=\left[\rho, \rho u, \rho v, e\right]^T ,$$

$$\mathbf{E}=\left[\rho u, \rho u^2+p, \rho uv, (e+p)u\right]^T, \quad \mathbf{F}=\left[\rho v, \rho uv, \rho v^2+p, (e+p)v\right]^T \quad , \tag{3}$$

with T denoting the transpose operator. The total energy per unit volume is defined as $e=p/(\gamma-1)+\rho\left(u^2+v^2\right)/2$ and $\gamma=c_p/c_v$ is the ratio of the specific heats, which is equal to 1.4 for air. In these equations, (u,v) are the velocity components in the (x, y) direction, ρ is the fluid density, and p is the pressure. The source term $\mathbf{S}_v$ in Equation (2) consists of the viscous flux derivative terms in which the viscous flux vectors, the stress components, and the heat fluxes are represented as

$$\mathbf{E}_v=\left[0, \tau_{xx}, \tau_{xy}, u\tau_{xx}+v\tau_{xy}+q_x\right]^T, \quad \mathbf{F}_v=\left[0, \tau_{xy}, \tau_{yy}, u\tau_{xy}+v\tau_{yy}+q_y\right]^T \quad , \tag{4}$$

$$\tau_{xx}=\frac{2}{3}\mu\left(2\frac{\partial u}{\partial x}-\frac{\partial v}{\partial y}\right), \quad \tau_{xy}=\mu\left(\frac{\partial u}{\partial y}-\frac{\partial v}{\partial x}\right), \quad \tau_{yy}=\frac{2}{3}\mu\left(2\frac{\partial v}{\partial y}-\frac{\partial u}{\partial x}\right) \quad , \tag{5}$$

where μ is the fluid viscosity and (q_x, q_y) are heat flux along the (x, y) direction, respectively. These equations can be made dimensionless by normalizing the variables using reference quantities such as $U_\infty, \rho_\infty, T_\infty, H$ and H/U_∞.

The laminar duct mean flow is developed from a uniform flow with velocity U_∞ and density ρ_∞ from far upstream, which creates a boundary layer on the top and bottom duct wall due to the action of fluid viscosity. The physical quantities H, U_∞ and ρ_∞ are chosen as the normalization parameters for the numerical simulations. The initial condition for the simulation adopts an incompressible Blasius flat-plate boundary layer profile along the duct walls. The initial momentum thickness at the leading edge of the cavity on the bottom wall is taken as $\theta_b/L=0.0189$ giving $\mathrm{Re}_{\theta_b}=\rho_\infty U_\infty \theta_b/\mu=56.8$. The same boundary layer is also specified on the top duct wall. Numerical results indicate that for configuration *BD* the variations of θ_b, as well as the top boundary layer profile, from their initial values are essentially constant during the course of simulation; therefore, the initial momentum thickness is used as one of the parameters of the problem. The Mach number far upstream $M=U_\infty/c_\infty$ is set equal to 0.4 where the ambient speed of sound is c_∞.

Equations (2) to (4) are solved using a sixth-order compact finite-difference scheme with a fourth-order Runge-Kutta time-advancement. This combination of schemes gives rise to a low dispersion and low-dissipative numerical method for resolving wave propagation accurately. A Cartesian grid is used for all simulations with fine clustering of grid points near the walls and in the shear layer regions spanning the cavities. Absorbing boundary conditions are applied in two buffer regions having widths $D_I/H = D_O/H = 1$ at the inlet and outlet of the duct in order to make sure that flow-generated acoustic waves are not reflected back into the computational domain. The setup of the absorption function within the buffer regions follows the same setup as that used in Leung et al. [4].

RESULTS AND DICUSSIONS

In one-step aeroacoustic simulation, the mean and fluctuating density, which contains both aerodynamic and acoustic components, are solved simultaneously. The acoustic fluctuations are usually at least three orders of magnitude weaker than their aerodynamic counterparts. For an accurate aeroacoustic analysis, one needs to distinguish these aerodynamic and acoustic fluctuations from the density solution. In the present study, the following approach is adopted. For all cases, the simulations are allowed to proceed until the solutions have reached time-stationary state. Afterwards, the mean density field is calculated by taking the time-average of the time-stationary solutions. The density fluctuations are then obtained by subtracting the mean field from the instantaneous one-step solution. As such, the stronger aerodynamic density disturbances are found localized near the cavity and duct walls and convect with the duct mean flow. The weaker acoustic density fluctuations are found propagating away from the cavity and dominate as plane waves near the duct inlet and outlet. The acoustic pressure and velocity fluctuations are also differentiated in the same fashion. Thus scrutinized, the acoustic analysis is performed in regions where aerodynamic fluctuations have completely decayed.

Figure 2 illustrates a snapshot of the distributions of vorticity and acoustic density fluctuations for the basic duct *BD*. The cavity flow is dominated by a shear-layer mode oscillation, in which the vortical disturbances propagate and grow along the shear layer, which does not separate but encloses the entire cavity (Figure 2a). A weak, relatively steady vortex occupies the downstream half of the cavity. The steadiness of the vortex suggests that the interaction of the flow inside the cavity with the shear layer is relatively weak; thus, the oscillation of the shear layer is largely responsible for the acoustic radiation. This observation is similar to the previous experimental study of an open cavity at a higher Mach number M = 0.64 by Krishnamurty [5]. It indicates that the dynamics of the shear layers and cavity vortex, which play dominant role in acoustic generation in open cavity studies [1–3], is not significantly changed in a flow duct situation. The boundary layer on the top wall is steady which further substantiates this observation. However, the frequency of the aeroacoustics is different due to the presence of the top duct wall. Spectral analysis of the transverse velocity v at the shear layer center $(x, y) = (1, 0)$ shows a dominant peak at $St_b = f_b H / U_\infty = 0.3849$. The frequency is 5% lower than the second mode oscillation of an open cavity at the same Mach number as predicted by the Rossiter formula [6]. The shear layer oscillation generates acoustic waves in both upstream and downstream directions (Figure 2b). It is evident that the acoustic waves become plane waves after they have propagated a distance $\approx 2H$. At $(x, y) = (6, 0)$ close to the duct outlet, the acoustic density fluctuates in a sinusoidal manner at the same St_b. The same frequency is also observed in the density fluctuation at $(x, y) = (-3, 0)$. These phenomena clearly show that the acoustic waves generated inside the duct is a direct consequence of cavity shear oscillation.

If the oscillation is modulated, the power of the acoustic waves could be reduced. In the present study, the modulation is provided by the introduction of an additional cavity into the top wall of the flow duct. The oscillation of the additional shear layer is allowed to interact with the bottom one with an aim to achieve an overall reduction of acoustic power. Figure 3 shows two proposals. The first one is to install another cavity with the same dimensions on the top duct wall opposite to the original cavity (*ECD*). The second proposal is to offset the additional cavity on the top duct wall by $L/2$ downstream of the original cavity (*OCD*). The initial and boundary conditions of the duct flow calculations of these two cases are the same as in the case of *BD*. The specification of the top boundary layer is the same as the bottom one.

Figure 4 shows a snapshot of the distributions of vorticity and acoustic density fluctuations for configuration *ECD*, which is commonly found in many muffler design for flow-induced noise mitigation. It is clear from Figure 2 that the two cavities interact strongly and give rise to a different shear layer dynamics. The shear layers no longer cover the cavities. Instead they roll up more quickly to form vortices (Figure 2a). Each vortex hits the cavity trailing edge and splits into two parts. One part is convected to the downstream boundary layer while another part is entrained into the cavity space to sustain the trapped vortex there. It is interesting to note that vortex shedding from the top and bottom cavities is asymmetric even though the duct geometry is symmetric about its axis along $y/H = 1$. For this configuration, the density fluctuations take slightly longer distance ($\approx \pm 3H$) to form plane acoustic waves towards the inlet and outlet. The density fluctuations at the leading and trailing edge are strong but are localised.

Figure 5 shows a snapshot of the distributions of vorticity and acoustic density fluctuations for configuration *OCD*. In this situation the two shear layers cover the cavities again but, in contrast with *BD*, no vortex is trapped in the cavity space. As a result the acoustic plane waves start to form at a shorter distance, $\approx \pm H$ compared to $\approx \pm 3H$ for the *ECD* configuration.

In the presence of a mean flow, the instantaneous acoustic intensity is generalized [7] as

$$\boldsymbol{I}(t) = p'\boldsymbol{u}' + (\boldsymbol{M} \cdot \boldsymbol{u}')(\boldsymbol{M}p' + \rho c \boldsymbol{u}') + \boldsymbol{M}\left(p'^2/\rho c\right) \quad , \tag{6}$$

where $\boldsymbol{M} = \overline{\boldsymbol{u}}/c$ is the local Mach number and the prime indicates acoustic quantities. For a general cross section far away from the cavities, the acoustic power W_a passing through this section can be defined as the integral of the acoustic intensity

$$W_a = \frac{1}{T}\int_0^T \int_0^2 \boldsymbol{I}(t)\,dydt \quad . \tag{7}$$

The acoustic power W_a at $x/H = -3$, +3 and +6 is evaluated and listed in Table 1. It is interesting to note that *BD* and *ECD* radiate the same power to the upstream and downstream direction. However, *OCD* radiates more towards the upstream than towards the downstream direction. On the other hand, for the three cases considered, addition of another cavity leads to a reduction of acoustic generation. Configuration *ECD* radiates ~6.3 db acoustic power reduction compared to that of *BD* in both upstream and downstream directions, while configuration *OCD* radiates ~7.9 db less in the downstream direction but only ~4.4 less in the upstream direction. From the forgoing discussion, the shear layer dynamics of *ECD* appears to be more violent than that observed in *BD* (Figure 4) but it eventually radiates less acoustic power. The observation might be explained by investigating the density fluctuations at the centers of the cavity openings. The root-mean-square density fluctuation $(\rho')_{rms}$ of *ECD* is in fact ~6 times stronger than that of *BD* (Table 2). However, the density fluctuations between the top and bottom cavity are almost out of phase. It gives rise to a very inefficient acoustic radiation in both the upstream and downstream direction due to the cancellation between two individual waves. One may note that such an out-of-phase relationship exists between the two shear layers in *OCD* and that causes the reduction of radiated acoustic power.

CONCLUSIONS

A numerical study of the aeroacoustics of multiple in-duct cavities in a flow duct is reported. The major objective is to verify the concept of passive noise reduction of overall noise generated from an in-duct cavity by introducing an additional one for the enhancement of noise interference. Two cavity arrangements are attempted. One is to put the additional cavity directly opposite to the original one (*ECN*) whereas another is to offset the additional cavity by one half cavity length (*OCN*). The numerical results show that the presence of the additional cavity in both arrangements is able to alter the cavity flow dynamics and consequently the noise radiating towards the duct inlet and outlet. Configuration *ECN* radiates noise equally towards the duct inlet and outlet with a power reduction of around 6.6 db. Configuration *OCN*, on the other hand, yields 4.4 db and 7.9 db noise power reduction towards the duct inlet and outlet, respectively.

ACKNOWLEDGEMENTS

Support from the Research Grants Council of the HKSAR Government under Projects PolyU 5174/02E and PolyU 1/02C and the Internal Competitive Research Grant of The Hong Kong Polytechnic University under Project A–PF32 is gratefully acknowledged.

REFERENCES

[1] Grace S.M., Dewar W.G., and Wroblewski D.E., "Experimental investigation of the flow characteristics within a shallow wall cavity for both laminar and turbulent upstream boundary layers". Expt. Fluids, **36**, 791-804, (2004)

[2] Larsson J., Davidson L., Olsson M., and Eriksson L.E., "Aeroacoustic investigation of an open cavity at low Mach number". AIAA J., **42**, 2462-2473, (2004)

[3] Rowley C.W., Colonius T., and Basu A.J., "On self-sustained oscillations in two-dimensional compressible flow over rectangular cavities". J. Fluid Mech., **455**, 315-346, (2002)
[4] Leung R.C.K., Li X.M., and So R.M.C., "Comparative study of nonreflecting boundary condition for one-step duct aeroacoustics simulation". AIAA J., **44**, 664-667, (2006)
[5] Krishnamurty K., "Acoustic radiation from two-dimensional rectangular cutouts in aerodynamic surface". NACA Technical Report-3487, (1955)
[6] Rossiter E.J., "Wind tunnel experiments on the flow over rectangular cavities at subsonic and transonic speeds". Aeronautical Research Council Reports and Memoranda 3438, (1964)
[7] Morfey, C. L. , Dictionary of Acoustics, Academic Press, London, 99 (2001).

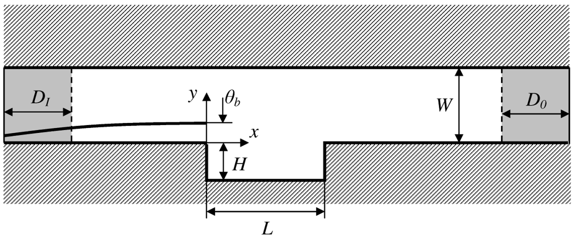

Figure 1. Configuration of the basic flow duct with an in-duct cavity (*BD*).

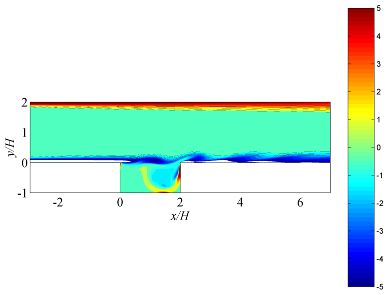

(a)

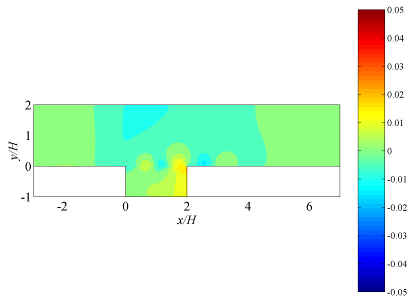

(b)

Figure 2. Aeroacoustics of flow duct with configuration *BD* at $U_\infty t/H = 17.5$: (a) normalized vorticity; (b) normalized density fluctuation ρ'/ρ_∞ .

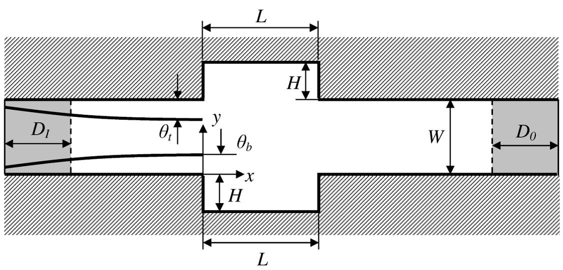

(a)

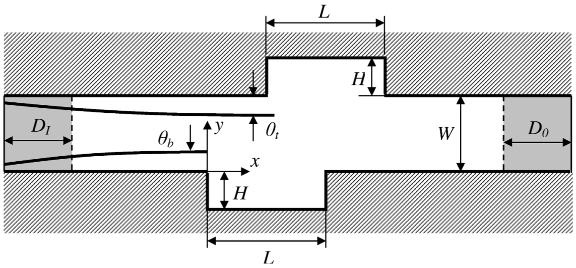

(b)

Figure 3. Configurations of the basic flow duct with two in-duct cavity: (a) *ECD*; (b) *OCD*.

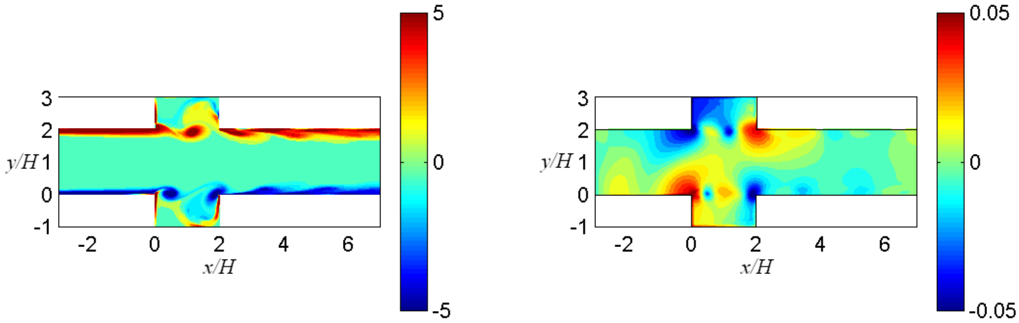

(a) (b)

Figure 4. Aeroacoustics of flow duct with configuration *ECD* at $U_\infty t/H = 10.3$: (a) normalized vorticity; (b) normalized density fluctuation ρ'/ρ_∞ .

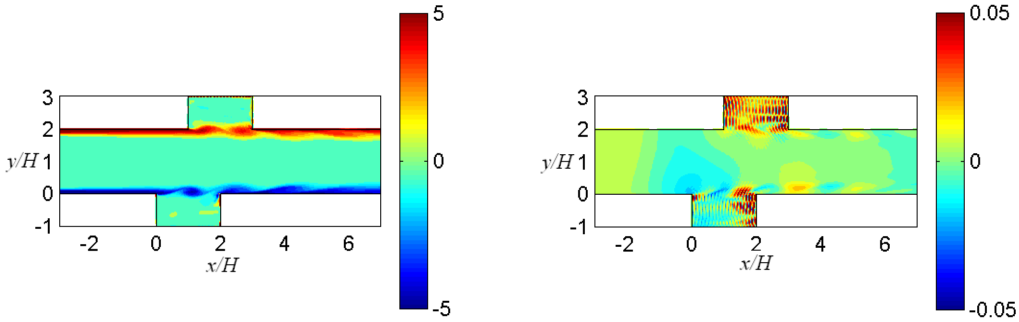

(a) (b)

Figure 5. Aeroacoustics of flow duct with configuration *OCD* at $U_\infty t/H = 10.3$. (a) Normalized vorticity; (b) normalized density fluctuation ρ'/ρ_∞ .

	$x/H = -3$	$x/H = +3$	$x/H = +6$
BD	0.179 (0 db)	0.179 (0 db)	0.179 (0 db)
ECD	0.043 (-6.2 db)	0.04 (-6.5 db)	0.041 (-6.4 db)
OCD	0.065 (-4.4 db)	0.039 (-6.6 db)	0.029 (-7.9)

Table 1. Normalized acoustic power at different streamwise location; brackets show the noise power level reduction using *BD* as reference.

	BD		*ECD*		*OCD*	
Top cavity	–	–	0.0649	-0.999π	0.0157	-0.9π
Bottom Cavity	0.0107	0	0.0649	0	0.0135	0

Table 2. Density fluctuations at the centers of shear layers. For each configuration, the first column shows the root-mean-square fluctuation and the second column shows the phases of fluctuations using the bottom cavity shear layer as reference.